Smith, R. B., and Y.-L. Lin, 1983: Orographic rain on Western Ghats. Mountain Meteorology, Ed. Reiter et al., Science Press and American Meteorology Society, 71-94.

1.4 OROGRAPHIC RAIN ON THE WESTERN GHATS

Ronald B. Smith and Yuhlang Lin
Department of Geology and Geophysics
Yale University
New Haven, Connecticut 06511 USA

ABSTRACT

The heavy monsoon rainfall along the Malabar Coast is clearly associated with influence of the Western Ghats yet, the primary source of the rain is deep convection rather than orographically forced ascent. To investigate this problem we combine an analytical treatment of thermally and orographically induced mesoscale circulations, with a steady state model of turbulent buoyant plumes. The results indicate that there are two internally consistent modes of airflow over the mountains. With no precipitation, the orographic disturbance is insufficient to destabilize the air column with regard to deep cumulus development. On the other hand, the disturbance produced by the heating computed from the observed rainfall, does alter the environment in such a way as to allow cumulonimbus development. This seems to offer a partial explanation for the rainy and dry spells on the coast observed during the summer monsoon. The existence of a heat-induced off-shore trough is also predicted by the model.

I. INTRODUCTION

A good example of the local enhancement of precipitation by orography is the large annual rainfall recorded along the Malabar Coast and on the windward slopes of the Western Ghats in India (Fig. 1). This rainfall occurs almost entirely during the 3-4 month summer period when the coast lies in the path of the west-southwest monsoon winds crossing the Arabian Sea. For the purpose of discussion, it is possible to identify five existing theories which might account for the observed rainfall.

1) Smooth uplift [25], [26], [27] in which the vertical motion leading to condensation and precipitation is directly forced by the upsloping terrain below.

2) Diurnal convection (e.g. [18]) in which the temperature difference between land and sea, or heated mountain slopes produce circulations which trigger the onset of convection each afternoon.

3) Coastal trough [6], [9], [14] which, like a synoptic scale trough in midlatitudes, is thought to be associated with rainy weather.

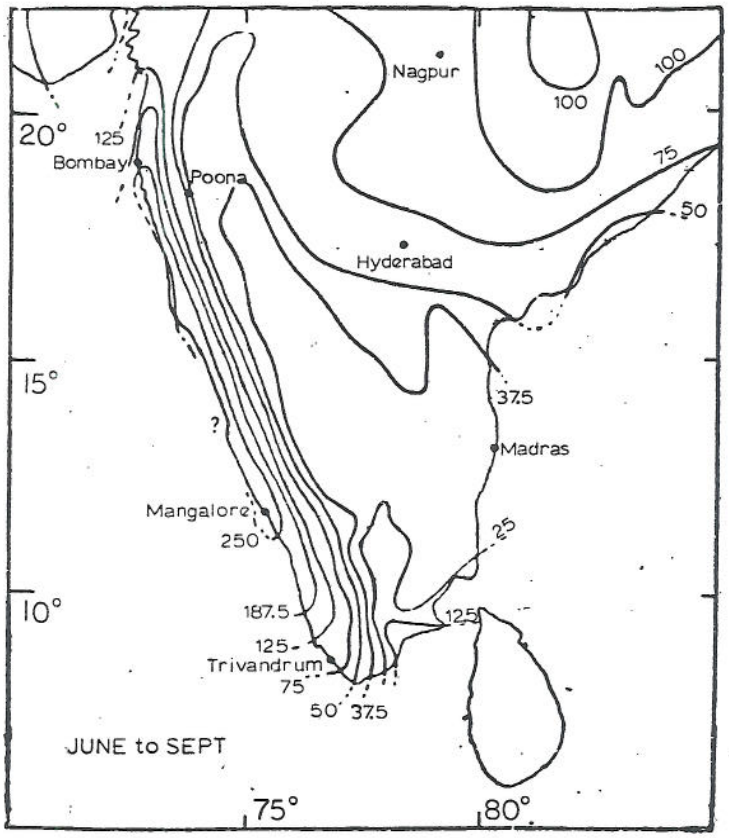

Fig. 1 The areal distribution of rainfall over India during the summer monsoon months of June to September (from [20]). The rainfall is concentrated just upstream of the Western Ghats. The seaward extent of the high rainfall region is not known.

4) Lifting instability (e.g. [5]) in which the orographic lifting triggers deep convection.

5) Low-level feeder clouds [1], [2] which redistribute the rainfall reaching the ground while not influencing the main hydrometeor production aloft.

While none of these theories can be said to be irrelevant to the problem at hand, there is contradictory evidence for each. The showery nature of the rainfall and the satellite observation that the rainfall is caused by deep cumulonimbus clouds seems to speak against (1) in its pure form but yet low-level forced orographic lifting along the lines of (5) is helping to enhance rainfall on local hills and to smooth out the showery fluctuations there. There is a measurable diurnal modulation to the rainfall,

supporting (2), but this is a minor effect in this particular region. The empirical association (3) between rainfall and a coastal trough is supported by the analysis in this paper, but the trough is seen to be a result of the rainfall rather than a cause. The widely discussed mechanism of destabilization by orographic lifting (4) seems to be most relevant here, yet the suggestion of this paper is that it needs a substantial modification. The mesoscale lifting that triggers the convection is largely produced by the latent heating itself, rather than the mountain. The rainfall system is then nearly self-sustaining, with the mountain acting only to stabilize the system and hold it in place.

In this paper we will construct a more detailed, but still semi-empirical, model of the Malabar Coast rainfall. From this model we conclude that of the four existing conceptual models, no. 4 is closest to the truth but that it is oversimplified. In fact the latent heating in the rainclouds generates instability much the way a propagating squall line might do. The somewhat smaller influence of the mountain serves to anchor the system and to maintain its organization. This behavior gives the system a discrete on-off character leading to rainy and dry spells.

II. THE MONSOON WIND

The structure of the summer winds approaching India has been studied for a number of years [10], [5], [11], [21], [23], [3]. Progress in this research has recently accelerated due to the observations from the MONEX project.

Throughout the summer monsoon period, the low-level winds across the Arabian Sea approach India with a speed of about 15 m/s (at 850 mb), and a direction more or less perpendicular to the coast (Fig. 2). Embedded in the flow are minor disturbances which account for variations in cloudiness over the sea and for a time-varying streakiness to the wind strength. In the upper troposphere, the winds are reversed, blowing from the east. Disturbances exist in these easterlies as well, and these may also play an important role in modulating rainfall in the region.

III. THE NATURE OF THE RAINFALL ALONG THE MALABAR COAST

As shown in Fig. 3, the land immediately along the coast receives considerable annual rainfall while the western slopes of the Ghats receive even more. Immediately beyond the crest of the mountains the rainfall decreases to a low value and this amount is mostly associated with tropical depressions approaching from the east. Based on estimates of rainfall far out over the sea, the coastal rainfall is at least thrice the upstream value. The lack of rainfall data just off the coast makes it difficult to estimate how far offshore the enhanced region extends. Rainfall estimates from satellite [22] may not be accurate enough to resolve this question. From limited radar data showing cumulus cloud development [31], it is likely that the enhancement extends at least 30 km offshore.

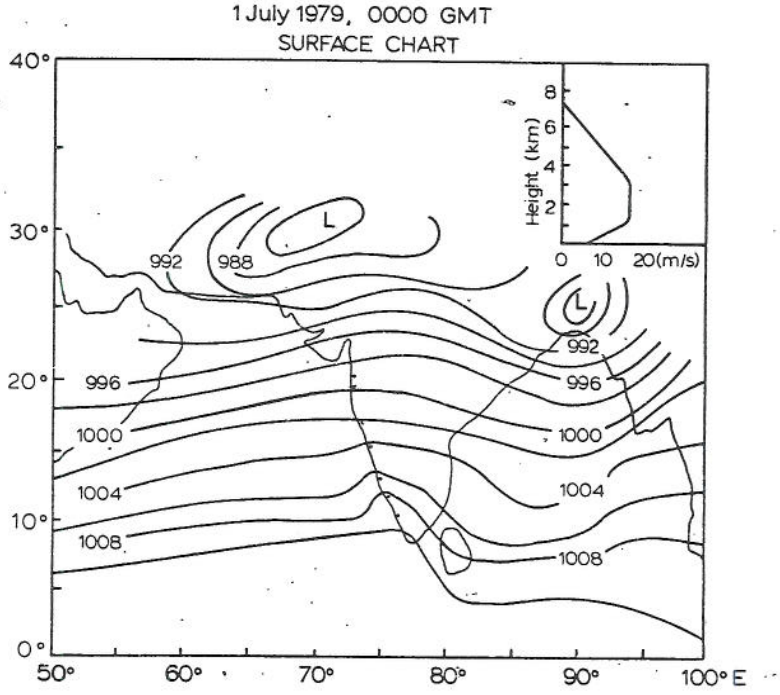

Fig. 2 A typical surface chart for the Indian Ocean during the summer monsoon. This particular chart is for 1 July 1979 at 0000 GMT. Also shown is a vertical sounding taken from the western coast of India showing the component of wind speed perpendicular to the coast. Above 7 km the winds are easterly.

Part (d) of Fig. 3 shows the distribution of rainfall across a section of the coast where mountains are broken by a gap (the Palghat Gap). The marked difference between this profile and the others is, in our view, that the gap is so narrow that it doesn't influence the enhanced shower development along the shoreline, but the local enhancement due to orographically forced low-level feeder clouds is missing.

Evidence that the origin of the rainfall is not smooth orographic lifting is quite clear. Local observations indicate that the rainfall is very irregular with adjacent 3-hour averages being almost uncorrelated, while the onshore winds continue unabated. Thus, in spite of the obvious importance of low-level feeder clouds, it seems that the ultimate cause of the rain is the development of deep convection.

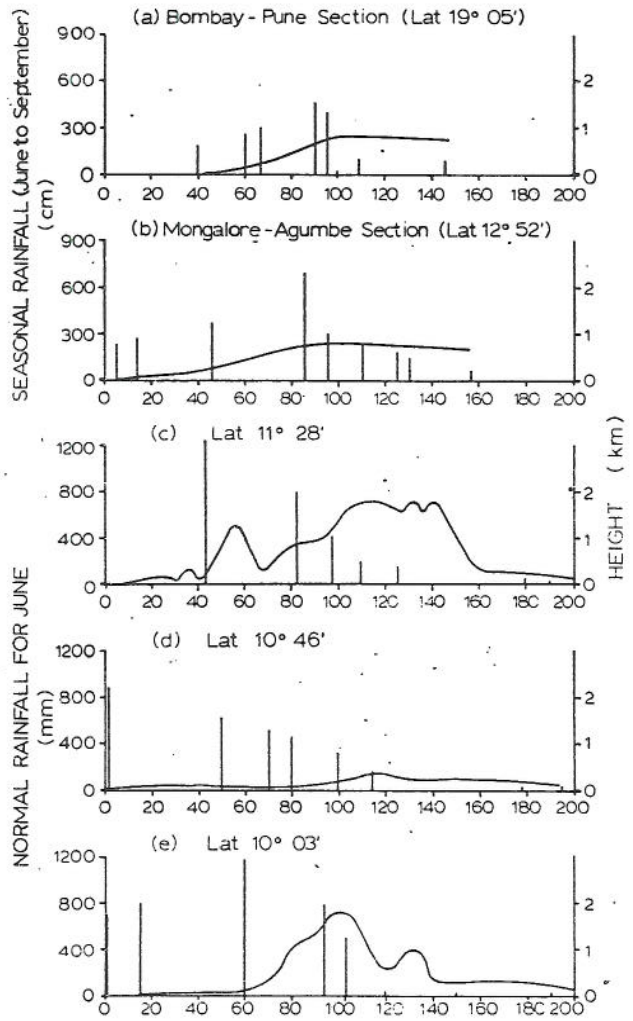

Fig. 3 The distributions of rainfall for several sections across the Western Ghats. (a) Bombay-Pune section with latitude about 19°05'. The seasonal rainfall of June to September (in cm) and mountain profile are plotted. (b) Same as (a), except for Mongalore-Agumbe section with latitude about 12°52'. (From [27].) (c) Cross section at latitude 11°28'. The normal rainfall for June (in mm) and mountain profile are plotted. (d) Cross section at latitude 10°46', through the Palghat gap. There is no increase of rainfall from the coast toward the eastern side. (e) Same as (c), except at latitude 10°03'. (From [17].).

From Fig. 4, and the more exhaustive survey shown in Fig. 5, it is evident that the showers occur in spells lasting 5-10 days separated by equally long dry spells. It is not known what aspects of the larger-scale environment control the spells. During the rainy spells, the average precipitation rate on the coast is usually between 2-4 mm/hr.

The diurnal variation in rainfall is shown in Fig. 6, both for the MONEX period and from a longer climatic record [15]. These data show a definite diurnal modulation yet the magnitude of the modulation is small. We conclude that unlike most tropical coastlines, the thermal forcing caused by land-sea or mountain-plain temperature differences is of minor importance along the Malabar Coast.

IV. THE GOVERNING EQUATIONS AND THE TWO-SCALE APPROXIMATION

In order to mathematically describe the local dynamics during the spells of heavy rain we split the flow field into three parts. First, the basic state is taken to be the steady undisturbed west-southwest monsoon flow [denoted by upper case symbols $U(z)$, $\theta(z)$]. Added to this is a steady-state mesoscale perturbation (denoted by primes) generated by the orography, and by the latent heat release in groups of cumulus clouds. Third, there are smaller-scale unsteady motions (denoted by double primes) associated with the individual cumulus clouds which can act collectively to influence the larger, mesoscale, field of flow. These quantities are defined such that $\overline{u''}$, $\overline{w''}$, $\overline{\theta''} \equiv 0$. In these equations, all the variables have their usual meanings (see [28]) except $\bar{Q}(x,z)$ which is defined as the rate of latent heat release per unit volume, and α, which is a coefficient of thermal expansion ($\alpha = 1$ for a perfect gas).

For the calculation of the mesoscale flow field the following assumptions are employed:

- small amplitude
- steady
- Boussinesq
- two-dimensional
- large Rossby number
- hydrostatic

within these assumptions the governing equations are

$$\rho_o U \frac{\partial u'}{\partial x} + \rho_o w' \frac{\partial U}{\partial z} = - p'_x - \rho_o \left\{ \overline{\frac{\partial u''^2}{\partial x}} - \overline{\frac{\partial u'' w''}{\partial z}} \right\} \qquad (1)$$

$$0 = -p'_z - \rho' g - \rho_o \left\{ \overline{\frac{\partial u'' w''}{\partial x}} - \overline{\frac{\partial w''^2}{\partial z}} \right\} \qquad (2)$$

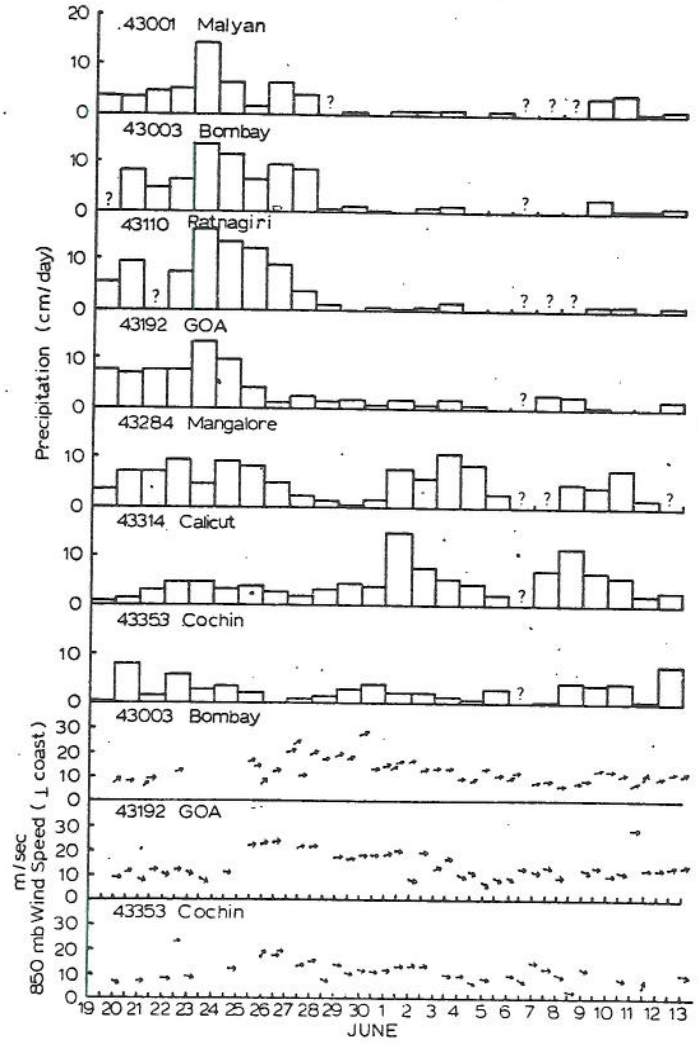

Fig. 4 A time series of daily rainfall amounts from seven stations along the Malabar Coast during the period 19 June to 13 July 1979. The stations are presented in order - north to south as shown in Fig. 2. Although the rainfall is convective in nature, the daily rainfall totals tend to be more continuous with rainy spells and dry spells extending over a substantial fraction of the coast. The bottom part of the figure shows the strength of the onshore winds from three coastal stations during the same period.

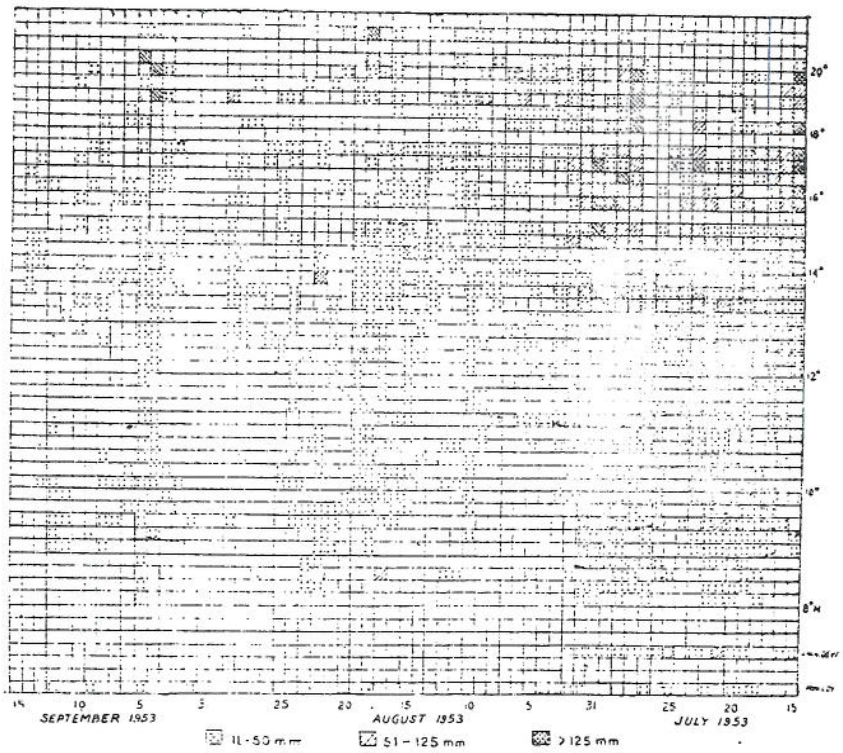

Fig. 5 Day-to-day rainfall variations along the Western Ghats and the Malabar Coast throughout the period from July to September 1953. Note that the spells of heavy rainfall persist for about 5-10 days separated by equally long dry spells. (From [20].)

$$\rho_o c_p \{U\frac{\partial \theta'}{\partial x} + w'\frac{\partial \theta}{\partial z}\} = \bar{\bar{L}} - \rho_o c_p \{\frac{\partial}{\partial z}\overline{\theta'' w''} - \frac{\partial}{\partial x}\overline{\theta'' u''}\} \tag{3}$$

$$\rho'/\rho_o = \alpha\theta'/\theta_o \tag{4}$$

$$\frac{\partial u'}{\partial x} + \frac{\partial w'}{\partial z} = 0 \tag{5}$$

The averages denoted by the overbar are, in principle, taken with respect to time as the mesoscale flow is independent of this variable. In practice however, additional averaging over small regions of space (e.g. $\Delta x \sim 10$ km, $\Delta z \sim 300$ m) would be necessary to obtain statistical significance. This in turn requires that the steady mesoscale flow and the unsteady cumulus dynamics are really occurring on two different scales. This is a crucial assumption and one that is difficult to defend.

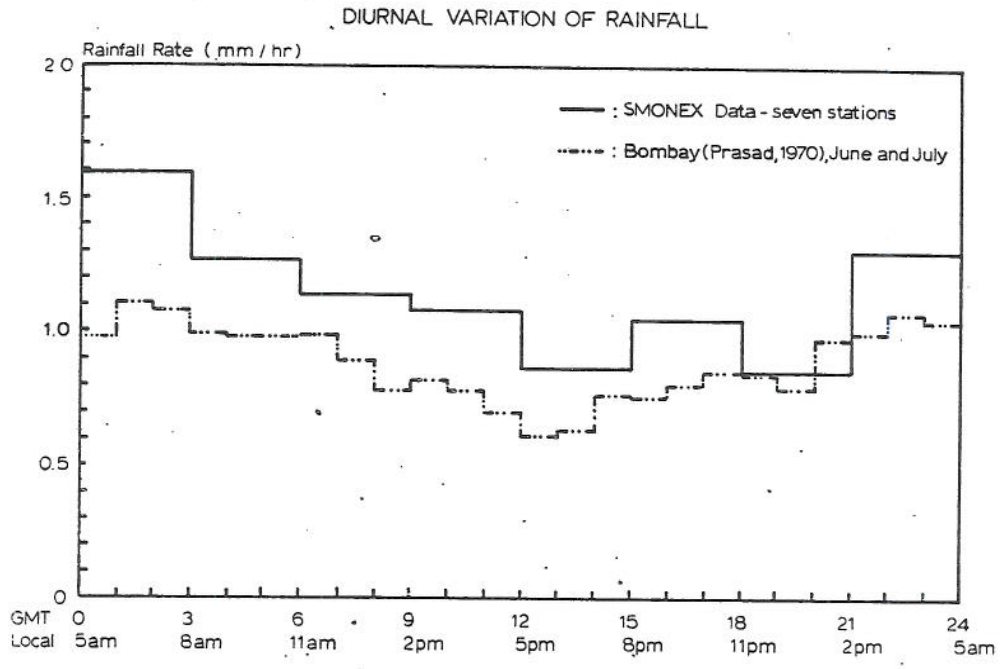

Fig. 6 Average rainfall rate (mm/hr) as a function of time of day. The solid curve is from 3-hourly data from the SMONEX data set. It includes data from the seven surface stations shown in Figs. 2 and 3, for the periods June 21 to July 6 and July 9 to July 13, 1979. The dashed line was calculated from hourly data from Bombay for the months of June and July, 1948-1965 by Prasad [15]. Both curves show a minor early morning maximum.

That this scale split is possible is suggested by the nature of local rainfall statistics. From a single station, a long record, perhaps longer than a "spell", is required to obtain a representive value for average rainfall rate. On the other hand, if several stations are included, especially similarly situated stations along the coast, then a representative rainfall rate can be obtained from a short time average (i.e. $\sim$ a few hours). This suggests that the effect of cumulus clouds can be considered as a statistically stationary forcing function over the period of a rainy spell.

The problem can be reduced to its most basic physical elements if we make the following further assumptions:

- neglect vertical shear in the background flow (Eq. 1)
- neglect the Reynolds stresses due to the cumulus clouds (Eqs. 1, 2)
- neglect the horizontal transport of sensible heat by the cumulus clouds (Eq. 3).

These assumptions are not required for mathematical tractability. Equations (1)-(5) can then be reduced to a single equation for w'(x,z) as follows:

$$w'_{zz} + \ell^2 w' = \frac{gH\alpha}{\rho_o c_p \theta_o U^2} \tag{6}$$

where

$$H(x,z) \equiv \bar{\bar{L}} + \rho_o c_p \overline{\frac{\partial \theta'' w''}{\partial z}} \tag{7}$$

is the combined effect of latent heat release and turbulent vertical heat transport in the cumulus clouds.

The appropriate boundary conditions are:

$$\text{at } z = 0 \qquad w' = U\frac{\partial h(x)}{\partial x} \tag{8}$$

where h(x) is the shape of the surface topography, while

$$\text{at } z \to \infty \qquad \text{Sommerfeld Radiation Condition} \tag{9}$$

The solutions to Eqs. (6), (8), and (9) with various choices for H(x,z) have been discussed by Smith and Lin [29], including the questions about vertical momentum flux, the phase relation between H and w', decay of the disturbance downstream, and the possibility of negative mountain drag. In this paper we will simply apply these results to the Western Ghats problem.

The most convenient closed-form solution arises from a heating function given by $H(x,z) = Q(x)/2d$ for $z_H + d\,\partial z > z_H - d$

$$\text{where} \quad Q(x) = Q\left(\frac{b_1^2}{(x+c)^2+b_1^2} - \frac{b_1 b_2}{(x+c)^2+b_2^2}\right) \tag{10}$$

and $H(x,z) = 0$ for $z > z_H + d$ and $0 > z > z_H - d$

and topography given by

$$h(x) = \frac{ha^2}{x^2+a^2} \tag{11}$$

In these formulae

Q is a measure of the strength of the vertically integrated heating ($Q = \max\{Q(x)\}$ if $b_2 >> b_1$)

z_H is the central altitude of the heating

d is the height above and below z_H to which the heating extends

b_1 is the half-width of the heating distribution

b_2 is the half-width of a compensating cooling required to keep the solutions bounded at infinity (normally $b_2 >> b_1$)

c is the horizontal distance between the center of the heating and the peak of the mountain

h is the height of the mountain

a is the half-width of the mountain.

The solutions for vertical displacement, pressure, and momentum flux associated with Eqs. (10) and (11) are given in the appendix. These expressions are rather lengthy because of all the geometric parameters that they include, but they can be easily plotted to investigate various combinations of orographic and thermal forcing.

V. THE DISTURBANCE TO THE MONSOON WIND BY THE COMBINED EFFECT OF OROGRAPHY AND CUMULUS HEATING

We first examine the disturbance caused by orography alone by plotting (in Fig. 7) the streamlines given by A1 with Q = 0. For the Western Ghats we choose h = 800 meter, a = 40 km, U = 10 m/s, $\ell = N/U = 0.001\ m^{-1}$. The result is the familiar pattern of vertically propagating mountain waves first presented by Queney [16]. Note that the lifting of the low-level air begins well upstream but we will see in a later section that this lifting is insufficient to trigger the growth of cumulus clouds. Between 3 and 4 kilometers there is orographically induced descent.

In order to estimate the value of H(x,z) we can integrate Eq. (7) vertically. If $\overline{\theta''w''}$ vanish as at z = 0 and ∞ then

$$Q(x) \equiv \int_0^\infty H(x,z)dz = \int_0^\infty \bar{L}(x,z)dz \qquad (12)$$

If we further assume that all the condensed water falls immediately to the ground, then from Eq. (12) and from the conservation of water mass

$$Q(x) = \lambda \overset{o}{R}(x) \qquad (13)$$

where λ is the latent heat of condensation per unit mass (2.5×10^6 J/kg) and $\overset{o}{R}(x)$ is the rainfall at the ground (kg/sec-m^2). Raingauge measurements of $\overset{o}{R}(x)$ allow us to estimate Q(x), but not the way in which the heat input is distributed in the vertical.

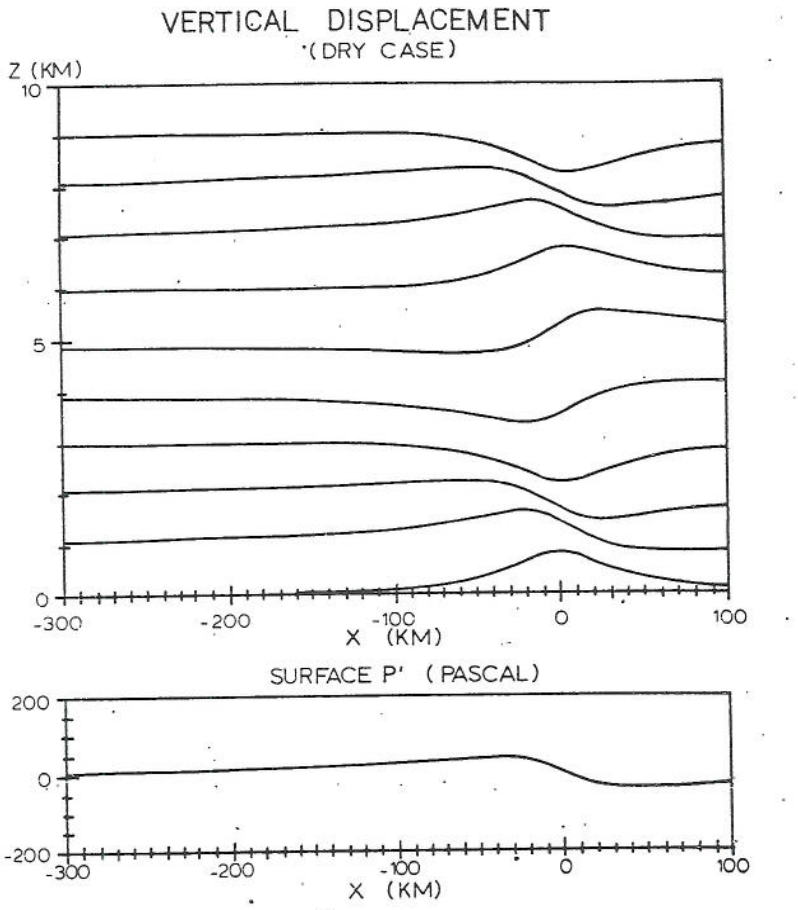

Fig. 7 Hydrostatic adiabatic flow over a bell-shaped mountain. The surface perturbation pressure is shown at bottom.

For the purpose of illustration we choose a maximum rainfall rate 1.7 mm/hr ($\sim 4.8 \times 10^{-4}$ kg/sec-m^2) which from Eq. (13) gives Q = 1200 W/m^2. Rather arbitrarily we choose z_H = 3 km and d = 1.5 km. This gives a maximum value of the local heating rate of H(x,z) = Q/2d = 0.4 W/m^3. From the horizontal distribution of rainfall we select b_1 = 40 km, b_2 = 200 km and c = 100 km. The results are shown in Fig. 8.

The comparison of Figs. 7 and 8 indicates that the heating is producing a disturbance which is at least as large as that of the mountain.

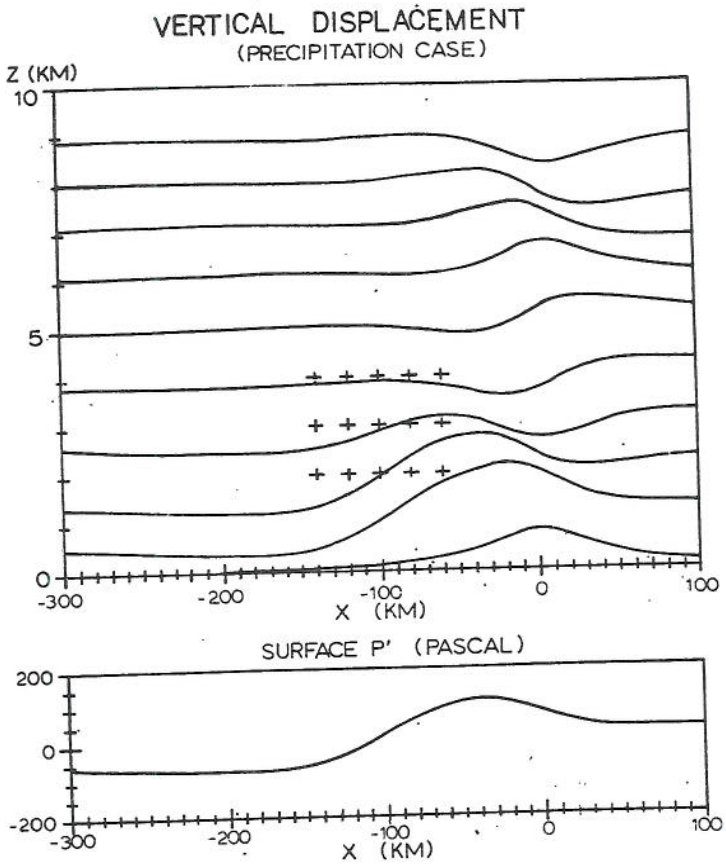

Fig. 8 Hydrostatic flow with combined thermal and orographic forcing. Isolated heating is specified over the area with "+". This flow is given by Eq. (A1) with Q = 1200 watts/m^2, b_1 = 40 km, b_2 = 200 km, a = 40 km, h = 0.8 km, c = 100 km, z_H = 3 km, d = 1.5 km, $\bar{U}$ = 10 m/s, N = 0.01 sec^{-1}. The maximum heating rate (at x = -100 km) corresponds to a rainfall rate of about 1 mm/hr. The surface perturbation pressure p' is drawn at the bottom. Note that there is a wide pressure trough produced by the heating, which is absent in the adiabatic case.

The nature of the thermally induced displacements are moderately sensitive to the choice of z_H (see [29] for a discussion of this point). For this choice (z_H = 3 km) there is a region of strong low-level convergence and ascent which may be able to trigger cumulus growth. This choice is reasonable as waves generated in the upper troposphere would be absorbed by the critical level in midtroposphere. Also, the condensation and sensible heat flux convergence in the upper troposphere may be largely offset by the evaporation of detrained liquid water.

VI. THE GROWTH OF CUMULUS CLOUDS

The analysis in the previous section was empirically based as the magnitude and position of the thermal forcing was estimated from observations of rainfall rate. It remains to be seen whether the calculated mesoscale flow field could lead to the vertical growth of small-scale cumulus clouds, which in turn would generate the assumed latent heat. Only if this is so, can we claim to have a self-consistent description of the orographic rain system.

To investigate this point we begin with an upstream sounding of temperature and dew point as obtained from an offshore island (see Fig. 9). Using the vertical displacements shown in Figs. 7 and 8, and working on a thermodynamic chart in the usual way, a new sounding can be calculated for each position downstream of original sounding (Fig. 8). The stability of these new soundings against moist convection can then be examined.

Unfortunately, the determination of the likelihood of cumulus growth is a rather difficult and uncertain business, although there is no lack of published literature on the subject. The parcel method, the slice method [8] and the various stability indices seemed to be of little use in this problem because they are not sensitive to changes in low- and mid-level relative humidity. As shown in Figs. 7 and 8 and then in Fig. 9, the primary result of the mesoscale lifting between z = 1 and 3 km is an increased relative humidity of this layer.

A more useful method seems to be the steady state moist plume model of the sort proposed by Morton [12] and by Squires and Turner [30]. Because of the vigorous lateral entrainment in this model, the growth of the plume is quite sensitive to the nature of the air it is penetrating. The entrainment of dry air from the sides will cause the evaporation of existing liquid water in the cloud and the subsequent loss of heat will cause the updraft to lose its buoyancy.

Of course the Squires and Turner [30] model is not completely reliable. Probably the most serious objection to it is the neglect of entrainment at the top of the cloud and the generation of cool downdrafts within the cloud [33], [4], [32]. For the present purposes we will accept the model in its original form (see Appendix II), in part because its behavior and shortcomings are well documented (e.g. its overestimation of vertical velocity) and in part because we think it may be accurate enough to give a reasonable comparison of stability between soundings which are not too different. Before applying the Squires-Turner model to the present problem, their test cases were redone to check both their computational methods and ours. Our calculations matched theirs to within a few percent.

The result of a steady state plume calculation on three environmental soundings is shown in Fig. 10. A moist plume starting at cloud base (z = 1 km) in the original sounding "A" will grow upwards at first due to latent heat release but will soon lose buoyancy as it enters the stable, drier air near 3 km. For this particular sounding, the plume is just barely able to penetrate into the less stable air near 4.5 km, where

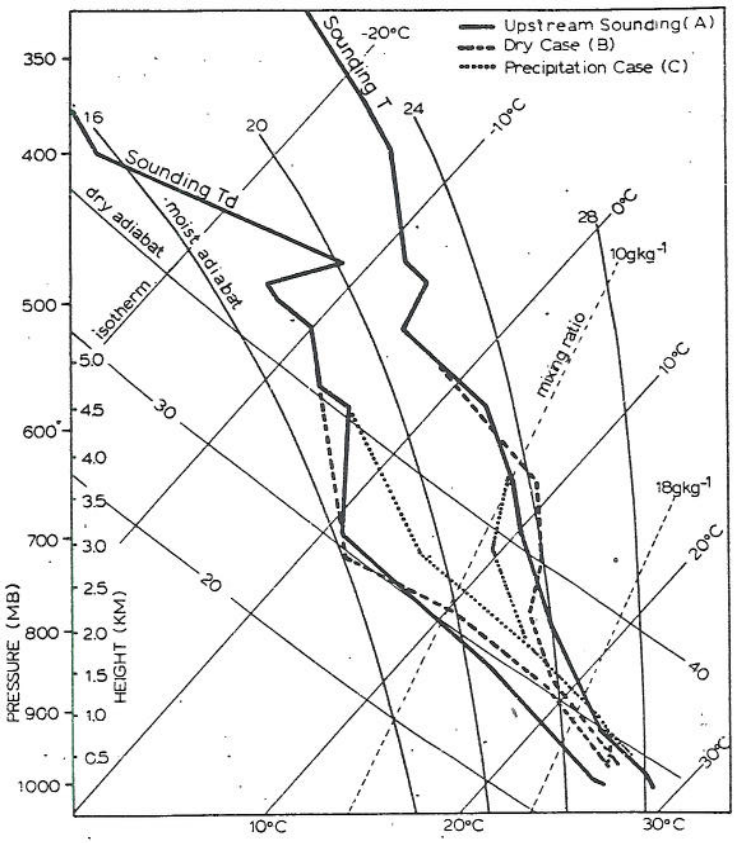

Fig. 9 A thermodynamic chart of the original upstream sounding, and the soundings modified by the vertical displacements shown in Figs. 7 and 8, at x = -100 km. The solid curves are the upstream sounding of temperature (T) and dew point (Td) at 0000 GMT, 1 July 1979 at Amihi which is about 300 km upstream. The dashed curves are the upstream sounding and modified by the mountain alone. The dotted curves are the upstream sounding and modified by the vertical displacements caused by the specified heating and mountain. The background lines are isotherms, dry and moist adiabats, and saturation mixing ratio.

it can reaccelerate. This seems consistent with the observation of frequent small cumulus clouds over the sea, which occasionally grew into cumulonimbus.

A similar calculation was done for sounding "B", representing the original sounding "A" modified by the dry flow field (Fig. 7). The result just above cloud base was much the same. At an altitude of 3 to 4

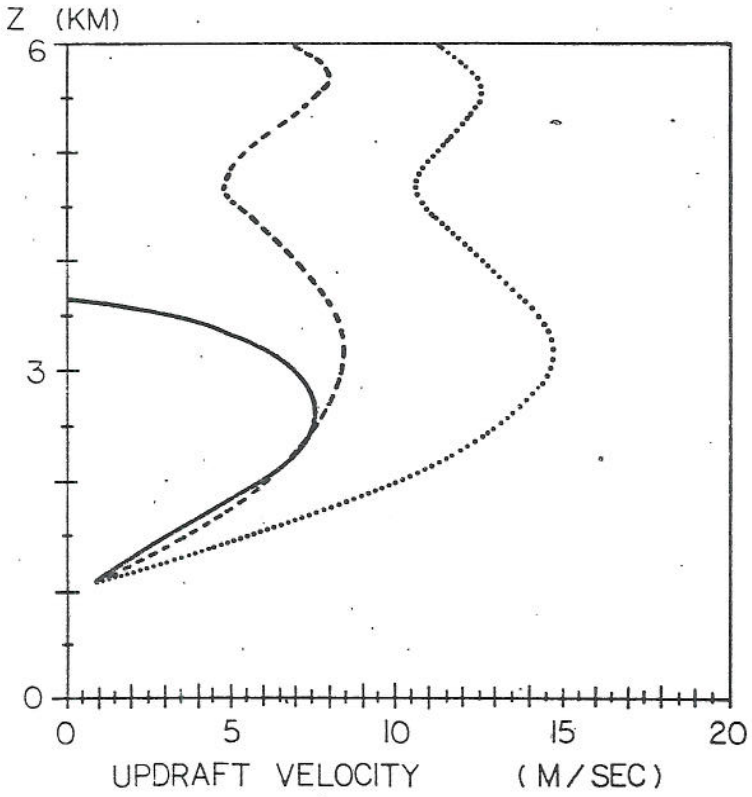

Fig. 10 The updraft velocity computed from a steady state plume model ([30]) using three environmental soundings (Fig. 8). The cloud base, initial updraft velocity and cloud base radius are assumed to be 1 km, 1 m/sec, and 1 km, respectively. The cloud base temperatures depend on the sounding and modified soundings. (a) The result of the calculation done using the original sounding (solid curve). (b) Adiabatic case (dashed curve), the sounding is modified by the orography as shown in Fig. 9. (c) Precipitation case (dotted curve), the sounding is modified by the orography and specified heating as shown in Fig. 9.

km, orographically forced descent has occurred and the increased stability prevents the vertical development of cumulus clouds.

The implication of this result is that the perturbation to the monsoon wind by the mountain alone may not be sufficient to destabilize the air column, it may even act to stabilize it against deep cloud growth. This is consistent with the occurrence of long dry spells during which the monsoon winds continued to blow against the coast and the mountains.

Finally, the plume model was run on sounding "C" - the original sounding modified by the flow field generated by combined heating and orography. In this case the environmental air above cloud base has been so strongly modified by mesoscale lifting that the plume can maintain its buoyancy and grow quickly to a significantly greater altitude. This result gives the self-consistency we mentioned earlier. The mesoscale perturbation computed from the observed heating rates, and with observed topography, is such as to destabilize the air column and allow cumulus to grow which could, in turn, produce the observed heat. There is also the suggestion that the perturbation from the heating alone - without the mountain - may be large enough to do this. Note in this regard that the plume model together with Eq. A1 (with h = 0) could describe a self-sustaining propagating squall line moving at a speed U over flat terrain.

VII. THE SURFACE PRESSURE FIELD

The trough of low pressure just upstream of the heating, illustrated in Fig. 8, is associated hydrostatically with a region of abnormally warm air aloft. This warm region is generated (according to Eq. 3) by direct heating and by heating induced subsidence. This trough is of interest for two reasons. First, something like it has been observed and reported by several authors and second, it raises the possibility (first suggested by Smith and Lin [29]) of a negative mountain drag.

Several authors [6], [9], [19], [14], [13] have discussed the observed association between heavy coastal rain and the existence of a mesoscale coastal trough as indicated by the low pressure at certain coastal stations. The structure of this "trough" offshore is not known. In these papers, the trough has been considered as an atmospheric disturbance which would produce heavy rain in much the same way as might a synoptic scale trough in midlatitudes. The possibility of using it as a forecasting tool has been discussed although it has not been possible to predict the occurrence of the trough.

Against this background, the current results offer a different interpretation. We find that the trough could arise as a result of the heating aloft rather than vice versa. Of course in the full model there is no cause-effect relationship because the downstream side of the trough is responsible for the low-level velocity convergence which triggers the cumulus growth. This theoretical result is consistent with the observation of Hoxit et al. [7].

It is clear that if the thermally induced surface low were strong enough and located over the windward slopes of the mountain, then a negative drag (or mountain thrust) would occur. This does not violate any fundamental principle as the latent heating represents an external energy source which allows the mountain to accelerate, rather than decelerate, the atmosphere passing over it.

We have looked at the predictions of the theory applied to the Western Ghats and at direct measurements of surface pressure in the region. Our results are somewhat inconclusive but seem to suggest that during heavy rain the thermal low is strong enough to reverse the drag

but that it is usually located too far upstream. Thus, while negative drag remains a real possibility, we can as of yet, offer no marked example.

VIII. DISCUSSION

In the preceding sections we have constructed a conceptual model of orographic rain. The number of assumptions involved in the analysis, and the lack of detailed data from the region, make it impossible to verify the model. It must remain, for the time being at least, a working hypothesis rather than a verified theory.

The most intriguing idea to come out of the model is the idea of multiple steady state solutions to the problem of moist airflow approaching a mountain range. We find internally consistent solutions both with and without rain. This seems to agree with the occurrence of wet and dry spells during the summer monsoon period. This implies that the system may have a bit of hysteresis, and that the question of how the system chooses between the two states might be a difficult one. We have not yet looked into the various subtle and not-so-subtle changes in the synoptic scale environment which could influence the system.

The discussion is also limited by the fact that we have not yet mathematically coupled the cumulus development with a time dependent mesoscale model. Only steady state solutions were considered herein. Until this is done we can say nothing about the stability of the system or how it might flip between the rain and no-rain states. Because the heating seemed to produce a slightly stronger mesoscale response than the orography, we tend toward a description of the orographic rain as a "squall line anchored to the mountain". A description of the "anchoring" process also requires a time dependent model with cumulus parameterization.

It may be that the mechanism described herein will find application on other tropical coastlines during periods of fresh onshore winds. In particular we find that the careful study of Sakakibara [24] concerning the cumulus development in the Kyushu region of Japan during southeast winds, to be very much in accord with the results reported herein for the Western Ghats.

ACKNOWLEDGMENTS

The discussions with C. Emanuel, R. Bleck, J. Klemp, C. Lord, D. Fitzjarrald, A.K. Mukherjee, U.S. De, D.R. Sikka, D. Durran, J. McGinley were helpful in the course of this research. Special thanks to D.R. Sikka for acting as host during a visit to the Indian Institute of Tropical Meteorology and to J. Fein of the National Science Foundation for making the visit possible. This research was supported in part by a grant (ATM 80-23348) from the Atmospheric Sciences Division of the National Science Foundation.

APPENDIX I

STEADY STATE PERTURBATIONS ON THE MEAN WIND

The vertical displacement produced by combined thermal and orographic forcing (Eqs. (10) and (11)) can be derived as (see [29])

$$\eta(x,z) = \eta_1(x,z) - A \sin \ell z \cdot \left[\left(\tan^{-1}\frac{x+c}{b_1} - \tan^{-1}\frac{x+c}{b_2}\right)\cdot\right.$$

$$\left.(\sin \ell(z_H+d) - \sin \ell(z_H-d)) - \frac{1}{2}\ell n\left(\frac{(x+c)^2+b_2^2}{(x+c)^2+b_1^2}\right)\cdot\right.$$

$$\left.(\cos \ell(z_H+d) - \cos \ell(z_H-d))\right],$$

$$\text{for } z < z_H-d$$

$$\eta(x,z) = \eta_1(x,z) + A\left[\cos \ell z \cdot \left(\tan^{-1}\frac{x+c}{b_1} - \tan^{-1}\frac{x+c}{b_2}\right) + \right.$$

$$\left.\frac{1}{2}\sin \ell z \cdot \ell n\left(\frac{(x+c)^2+b_2^2}{(x+c)^2+b_1^2}\right)\right](\cos \ell z - \cos \ell(z_H-d)) - A \sin \ell z$$

$$\left[\left(\tan^{-1}\frac{x+c}{b_1} - \tan^{-1}\frac{x+c}{b_2}\right) \cdot (\sin \ell(z_H+d) - \sin \ell z) - \right.$$

$$\left.\frac{1}{2}\ell n\left(\frac{(x+c)^2+b_2^2}{(x+c)^2+b_1^2}\right)(\cos \ell(z_H+d) - \cos \ell z)\right],$$

$$\text{for } z_H-d < z < z_H + d$$

$$\eta(x,z) = \eta_1(x,z) + A\left[\cos \ell z \cdot \left(\tan^{-1}\frac{x+c}{b_1} - \tan^{-1}\frac{x+c}{b_2}\right) + \right.$$

$$\left.\frac{1}{2}\sin \ell z \cdot \ell n\left(\frac{(x+c)^2+b_2^2}{(x+c)^2+b_1^2}\right)\right](\cos \ell(z_H+d) - \cos \ell\,(z_H-d))$$

$$\text{for } z > z_H + d \qquad \text{(A1)}$$

where $\eta_1(x,z)$ and A are defined as

$$\eta_1(x,z) = \frac{ha(a \cos \ell z - x \sin \ell z)}{x^2 + a^2}$$

$$A = \frac{gQb_1}{2d\rho_o c_p \bar{T} U^3 \ell^2}$$

The surface perturbation pressure at the ground can be computed from Eq. (A1) and using Bernoulli's equation

$$P'(x,o) = - \rho_o U\, u'(x,o) = \rho_o U^2 \left.\frac{\partial \eta}{\partial z}\right|_{z=0}$$

The result is

$$P'(x,o) = - \frac{\rho_o U^2 ha\ell x}{x^2+a^2} - A\ell \cdot \left[\left(\tan^{-1}\frac{x+c}{b_1} - \tan^{-1}\frac{x+c}{b_2}\right)\cdot\right.$$

$$(\sin \ell(z_H+d) - \sin \ell(z_H-d)) - \frac{1}{2}\ell n\left(\frac{(x+c)^2+b_2^2}{(x+c)^2+b_1^2}\right) \cdot$$

$$\left.(\cos \ell(z_H+d) - \cos \ell(z_H-d))\right] \qquad (A2)$$

The momentum flux can be computed from

$$F = \rho_o \int_{-\infty}^{\infty} u'w'\, dx$$

The solution associated with Eq. (A1) is

$$F = - \frac{\pi}{4}\rho_o h^2 NU - \pi A\ell\rho_o U^2 ha\left[\left(\frac{a+b_1}{(a+b_1)^2+c^2} - \frac{a+b_2}{(a+b_2)^2+c^2}\right)\cdot\right.$$

$$(\sin \ell(z_H+d) - \sin \ell(z_H-d)) + \left(\frac{c}{(a+b_1)^2+c^2} - \frac{c}{(a+b_2)^2+c^2}\right) \cdot$$

$$\left.(\cos \ell(z_H+d) - \cos \ell(z_H-d))\right]$$

$$\text{for } z < z_H-d$$

$$F = - \frac{\pi}{4}\rho_o h^2 NU - \pi A^2 \ell\rho_o U^2 (\cos \ell(z_H+d) - \cos \ell(z_H-d) \cdot$$

$$(\cos \ell z - \cos \ell(z_H-d))\, \ell n\left(\frac{(b_1+b_2)^2}{4\, b_1 b_2}\right) - \pi\, A\ell\rho_o U^2 ha \cdot \cdot$$

$$\left[\left(\frac{a+b_1}{(a+b_1)^2+c^2} - \frac{a+b_2}{(a+b_2)^2+c^2}\right)(\sin \ell(z_H+d) - \sin \ell z) +\right.$$

$$\left(\frac{c}{(a+b_1)^2+c^2} - \frac{c}{(a+b_2)^2+c^2}\right)\left(\cos \ell(z_H+d) - 2\cos \ell(z_H-d) + \cos \ell z\right)]$$

$$\text{for } z_H-d < z < z_H + d$$

$$F = -\frac{\pi}{4}\rho_o h^2 NU - \pi A^2 \ell \rho_o U^2 (\cos \ell(z_H+d) - \cos \ell(z_H-d))^2 \cdot$$

$$\ell n\left(\frac{(b_1+b_2)^2}{4\, b_1 b_2}\right) - 2\pi A \ell \rho_o U^2 ha(\cos \ell(z_H+d) - \cos \ell(z_H-d)) \cdot$$

$$\left(\frac{c}{(a+b_1)^2+c^2} - \frac{c}{(a+b_2)^2+c^2}\right)$$

$$\text{for } z > z_H + d \qquad \text{(A3)}$$

APPENDIX II

AN ENTRAINING JET MODEL

The method described by Squires and Turner [30] uses the following equations to describe a steady state entraining jet.

$M = b^2 u\rho$	mass flux definition
$\frac{d}{dz}M = 2b\alpha u\rho_o$	conservation of mass
$\frac{d}{dz}(Mu) = gb^2(\rho_o - \rho - \rho\sigma)$	conservation of momentum
$\frac{d}{dz}(M\sigma) + \frac{d}{dz}(Mq) = q_o \frac{dM}{dz}$	conservation of total water.

In these equations the quantities

b	plume radius
u	updraft velocity
ρ	plume density
α	entrainment coefficient ($\alpha = 0.10$)
ρ_o	environment density
g	acceleration of gravity
σ	specific liquid water
q	specific humidity of plume
q_o	specific humidity of environment

are functions of height (z). In addition, the perfect gas law, an energy equation, and the Clausius-Clapeyron equation are needed to complete the

system. For each calculation it is necessary to specify the environmental $\rho_o(z)$, $q_o(z)$ or equivalent, and the initial values for b, z, u at cloud base. In most cases it is sufficient to take the plume virtual temperature as equal to that of the environment at cloud base.

REFERENCES

1. Bergeron, T.: Studies of the orogenic effect on the areal fine structure of rainfall distribution. Met. Inst., Uppsala University, Rep. No. 6 (1968).

2. Browing, K.A.: Structure, mechanism and prediction of orographically enhanced rain in Britain. In Orographic Effects in Planetary Flows, GARP Publication Series #23, WMO, Geneve (1980).

3. Cadet, D. and H. Ovarlez: Low-level airflow circulation over the Arabian Sea during the summer monsoon as deduced from satellite-tracked superpressure balloons. Part I: Balloon trajectories. Quart. J. Roy. Met. Soc., 102, 805-816 (1976).

4. Cotton, W.R.: On parameterization of turbulent transport in cumulus clouds. J. Atmos. Sci., 32, 548-564 (1975).

5. Das, P.K.: The monsoon. St. Martin's Press Inc., New York, 162 pp (1972).

6. George, P.A.: Effects of off-shore vortices on rainfall along the west coast of India. Indian J. Met. Geophys., 7, 225-240 (1956).

7. Hoxit, L.R., C.F. Chappell and J.M. Fritsch: Formation of mesoslows or pressure troughs in advance of cumulonimbus clouds. Mon. Wea. Rev., 104, 1419-1428 (1976).

8. Iribarne, J.V. and W.L. Godson: Atmospheric thermodynamics. D. Reidel Pub. Co., Holland, 222 pp (1973).

9. Jayaram, M.: A preliminary study of an objective method of forecasting heavy rainfall over Bombay and neighborhood during the month of July. Indian J. Met. Geophys., 16, 557-564 (1965).

10. Krishnamurti, T.N. and Vince Wong: A planetary boundary-layer model for the Somali jet. J. Atmos. Sci., 36, 1895-1907 (1979).

11. Krishnamurti, T.N., Philip Ardanuy, Y. Ramanathan and Richard Pasch: On the onset vortex of the summer monsoon. Mon. Wea. Rev., 109, 344-363 (1981).

12. Morton, B.R.: Buoyant plumes in a moist atmosphere. J. Fluid Mech., 2, 127-144 (1957).

13. Mukherjee, A.K.: Dimension of an "off-shore vortex" in East Arabian Sea as deduced from observations during MONEX 1979. In Results of Summer MONEX Field Phase Research (Part A), FGGE Op. Rep. 9, WMO, Geneva, G. Grassman (ed.), 176-183 (1980).

14. Mukherjee, A.K., M.K. Rao and K.C. Shah: Vortices embedded in the trough of low pressure off Maharashtra-Goa coasts during the month of July. Indian J. Met. Hydrol. Geophys., 61-65 (1978).

15. Prasad, B.: Diurnal variation of rainfall in India. Indian J. Met. Geophys., 21, 443-450 (1970).

16. Queney, P.: The problem of airflow over mountains. A summary of theoretical studies. Bull. Amer. Met. Soc., 29, 16-26 (1948).

17. Ramachandran, G.: The role of orography on wind and rainfall distribution in and around a mountain gap: Observational study. Indian J. Met. Geophys., 23 (1), 41-44 (1972).

18. Ramage, C.S.: Monsoon meteorology. Academic Press, New York, 296 pp. (1971).

19. Ramakrishnan, A.R.: On the fluctuations of the west coast rainfall during the southwest monsoon of 1969. Indian J. Met. Geophys., 23, 231-234 (1972).

20. Ramakrishnan, K.P. and B. Gopinatha Rao: Some aspects of the non-depressional rain in peninsular India during the southwest monsoon. In Symposium on the Monsoon World, Indian Meteorological Department (1958).

21. Rao, G.V., W.R. Schaub, Jr. and J. Puetz: Evaporation and precipitation over the Arabian Sea during several monsoon seasons. Mon. Wea. Rev., 109, 364-370 (1981).

22. Rao, M.S.V. and J.S. Theon: New features of global climatology revealed by satellite derived oceanic rainfall maps. Bull. Amer. Met. Soc., 58, 1285-1288 (1977).

23. Saha, K.R. and S.N. Bavadekar: Moisture flux across the west coast of India and rainfall during the southwest monsoon. Quart. J. R. Met. Soc., 103, 370-374 (1977).

24. Sakakibara, H.: Cumulus development on the windward side of a mountain range in convectively unstable air mass. J. Met. Soc. Japan, 57, 341-348 (1979).

25. Sarker, R.P.: A dynamical model of orographic rainfall. Mon. Wea. Rev., 94, 555-572 (1966).

26. Sarker, R.P.: Some modifications in a dynamical model of orographic rainfall. Mon. Wea. Rev., 95, 673-684 (1967).

27. Sarker, R.P., K.C. Sinha Ray and U.S. De: Dynamics of orographic rainfall. Indian J. Met. Hydrol. Geophys., 29, 335-348 (1978).

28. Smith, R.B: The influence of mountains on the atmosphere. Advances in Geophysics, 21, 87-230 (1979).

29. Smith, R.B. and Y.L. Lin: The addition of heat to a stratified airstream with application to the dynamics of orographic rain. Quart. J. R. Met. Soc., 108, 353-378 (1982).

30. Squires, P. and J.S. Turner: An entraining jet model for cumulonimbus updrafts. Tellus, 14, 422-434 (1962).

31. Srivastava, G.P., B.B. Huddar and V. Srinivasan: Radar observations of monsoon precipitation. Indian J. Met. Geophys., 17, 249-252 (1966).

32. Telford, J.W.: Turbulence, entrainment, and mixing in cloud dynamics. Pageoph., 113, 1067-1084 (1975).

33. Warner, J.: On steady-state one-dimensional model of cumulus convection. J. Atmos. Sci., 22, 1035-1040 (1970).